

Probing the antikaon potential by K^-A elastic scattering*

A. Sibirtsev and W. Cassing
Institute for Theoretical Physics,
University of Giessen, D-35392 Giessen, Germany
(March 26, 2018)

We extract the antikaon potential from differential data on elastic K^-A scattering within Glauber theory at an antikaon momentum of 800 MeV/c. The K^-N cross section at densities up to 0.1 fm^{-3} is found to be close to the value given in free space K^-p and K^-n interactions (averaged over the number of protons and neutrons) whereas the ratio α of the real to imaginary part of the forward scattering amplitude $f(0)$ differs from the ratio α in free space indicating a dropping of $Re f(0)$ at finite nuclear density. The extrapolated K^- potential at a momentum of 0.8 GeV/c amounts to ≈ -28 MeV at density ρ_0 which is substantially less than the values extracted from kaonic atoms at zero momentum or heavy-ion data at $300 \text{ MeV}/c \leq p_K \leq 600 \text{ MeV}/c$. We, furthermore, investigate the perspectives of scattering experiments on ^{12}C at low ($\approx 300 \text{ MeV}/c$) and high ($\approx 1.2 \text{ GeV}/c$) momenta.

I. INTRODUCTION

Since the pioneering work of Kaplan and Nelson [1], that predicted large attractive antikaon self-energies in nuclear matter, speculations about strange condensates in neutron stars and relativistic heavy-ion collisions have raised the interest in kaon-nuclear physics [2–5]. These ideas have been supported by the data on kaonic atoms that indicate a strong attractive potential at zero antikaon momentum [6,7]. On the other hand, also the data on K^- production from heavy-ion collisions [8–12] have been interpreted in terms of a dropping antikaon mass at finite density [13–17]. Whereas the analysis [6,7] of the kaonic atom data suggests an attractive antikaon potential of ≈ -180 MeV at normal nuclear density, the data on K^- production from heavy-ion collisions lead to a potential $\approx -80 \div 120$ MeV [13–17]. This discrepancy might be attributed [18,19] to the momentum dependence of the antikaon potential, since the kaonic atoms explore stopped antikaons with $p_K \approx 0$, while the heavy-ion experiments have probed the range $300 \leq p_K \leq 600 \text{ MeV}/c$.

Among the available experimental methods the elastic and inelastic hadron-nucleus scattering are a traditional way [20] to study the optical potential. Moreover, by measuring the hA scattering at different projectile mo-

menta one can also evaluate the momentum-dependence of the potential. Here we study the possibility to measure the K^- optical potential by elastic K^-A scattering, analyze the available data and discuss the perspectives of K^- -meson scattering experiments at low and high momenta.

II. GLAUBER APPROXIMATION

The elastic scattering of an energetic hadron from a nucleus can be described by the Glauber theory of diffractive scattering as formulated in the Boulder Lectures in Theoretical Physics [20]. Here we refer to the final results from Ref. [20] and present the formulas relevant for the further calculations and discussions.

When neglecting the Coulomb distortion of the projectile the amplitude for the elastic scattering of the particle from the nucleus is given as

$$F_{el}(q) = ik \int_0^\infty J_0(bq) (1 - \exp[i\chi_N(b)]) b db, \quad (1)$$

where q is the momentum transferred from the projectile to the nucleus, k is the missile momentum, while J_0 is the zero'th order Bessel function. The phase shift χ_N may be approximated by

$$\chi_N(b) = \frac{2\pi f(0)}{k} \int_{-\infty}^\infty \rho(b, z) dz, \quad (2)$$

where $f(0)$ is the complex amplitude for the forward scattering of the projectile on a proton or neutron in the nucleus, while $\rho(r=\sqrt{b^2+z^2})$ is the nuclear density distribution. In principle, $f(0)$ should be given by the (density dependent) in-medium amplitude, but within the impulse approximation [21] it can be approximated by the forward scattering amplitude in free space. Via the optical theorem, furthermore, the imaginary part of $f(0)$ can be expressed in terms of the total particle-nucleon cross section σ as

$$Im f(0) = \frac{k}{4\pi} \sigma. \quad (3)$$

Introducing $\alpha = Re f(0)/Im f(0)$ the phase (2) might be rewritten as

$$\chi_N(b) = \sigma \frac{\alpha + i}{2} \int_{-\infty}^\infty \rho(b, z) dz. \quad (4)$$

*Supported by Forschungszentrum Jülich

The experimental results on the elastic differential cross section given by

$$\frac{d\sigma}{d\Omega} = |F_{el}(q)|^2 \quad (5)$$

(with $q=2k \sin(\theta/2)$) can be used for the evaluation of the cross section σ and the ratio of the real to imaginary forward scattering amplitude α . Recall, that σ and α might differ from the relevant values given in free space; a question that has to be discussed separately. Neglecting such modifications for a while, the traditional Glauber approximation thus allows to evaluate the in-medium parameters describing the interaction of the projectile with a finite nucleus.

Furthermore, the Coulomb correction may be taken into account by adding the Coulomb phase shift to the nuclear phase as proposed in Refs. [22–26]. The Coulomb corrected nuclear elastic scattering amplitude then is given by

$$F_{el}(q) = F_C(q) + ik \int_0^\infty J_0(bq) \exp[i\chi_C(b)] \times (1 - \exp[i\chi_N(b) + i\chi(b)]) b db. \quad (6)$$

The amplitude F_C and the phase shift χ_C describe the scattering by a point charge Z ,

$$F_C(q) = -\frac{2\xi k}{q^2} \exp[i\phi_C], \quad \chi_C(b) = 2\xi \ln(kb), \quad (7)$$

where

$$\phi_C = -2\xi \ln \frac{q}{2k} + 2\eta, \quad \xi = -\frac{Ze^2 m}{k \hbar c}, \quad \eta = \text{arg} \Gamma(1+i\xi). \quad (8)$$

The sign of ξ is given by the attractive (negative) or repulsive (positive) interaction of the projectile with the Coulomb field.

The phase shift χ in Eq. (6) is given by

$$\chi = \frac{8\pi\xi}{A} \int_b^\infty \rho(r) \left(\ln \left[\frac{1 + \sqrt{1 - \tau^2}}{\tau} \right] - \sqrt{1 - \tau^2} \right) r^2 dr, \quad (9)$$

with $\tau = b/r$ while $\rho(r)$ is the charge distribution.

We assume the charge density in Eq. (9) to be proportional to the nuclear density function in Eq. (2), which is normalized to the total number of nucleons A . For $4 \leq A \leq 16$ nuclei - to a good approximation - it is given by [26]

$$\rho(r) = (R\sqrt{\pi})^{-3} \left[4 + \frac{2(A-4)r^2}{3R^2} \right] \exp[-r^2/R^2], \quad (10)$$

with $R = \sqrt{2.5}$ fm for ^{12}C . For $A > 16$ nuclei the nuclear density is replaced by the Wood-Saxon distribution

$$\rho(r) = \frac{\rho_0}{1 + \exp[(r-R)/d]} \quad (11)$$

with

$$R = 1.28A^{1/3} - 0.76 + 0.8A^{-1/3} \text{ fm}, \quad d = \sqrt{3}/\pi \text{ fm}. \quad (12)$$

We note that we do not account for a screening phase and discard nucleus recoil corrections [25,26].

III. DATA ANALYSIS

The data on the differential cross section for the K^- -meson elastic scattering by ^{12}C and ^{40}Ca at an antikaon momentum of 800 MeV/c have been collected by Marlow et al. [27] and fitted by Eq. (6) in order to evaluate the cross section σ and real to imaginary ratio α . We here use the Minuit [28] procedure and the χ^2 method. The solid lines in Figs. 1,2 show the result from the minimization procedure together with the experimental results [27]. The parameters σ and α as well as the reduced χ^2 are listed in Table I.

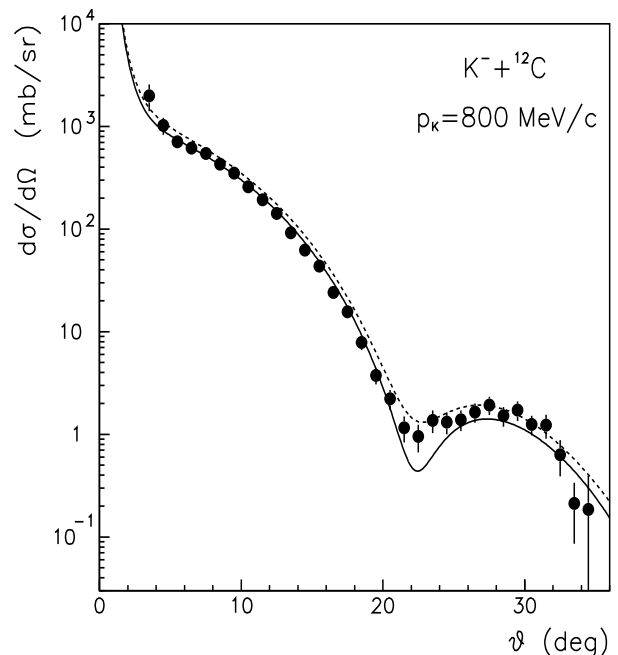


FIG. 1. The elastic differential cross section for K^- scattering from ^{12}C . The data are from Ref. [27]. The solid line shows the result from the fit with the parameters listed in Table. I while the dashed line indicates the calculations with σ and α taken from K^-N scattering in free space averaged over protons and neutrons in the target.

The dashed lines in Figs. 1,2 show the calculations with σ and α taken from the K^-p and K^-n interactions in free space and averaged over the number of protons and neutrons in the target as described below. We note, that

although the calculations with the free space variables provide a better description in the vicinity of the diffractive minima, they lead to a substantially worse χ^2/N as shown in Table I.

One of the crucial questions now is the sensitivity of the data to the sign and the magnitude of the ratio α . It is known [20] that - while σ is given by the absolute value of the nuclear cross section - the ratio α may be fixed by the differential cross section at the diffractive minima. Actually, any effect providing a complex correction of the nuclear scattering amplitude F_{el} influences the filling of the diffractive minima [26,29].

χ^2/N 1.4 1.7 5.1 4.3

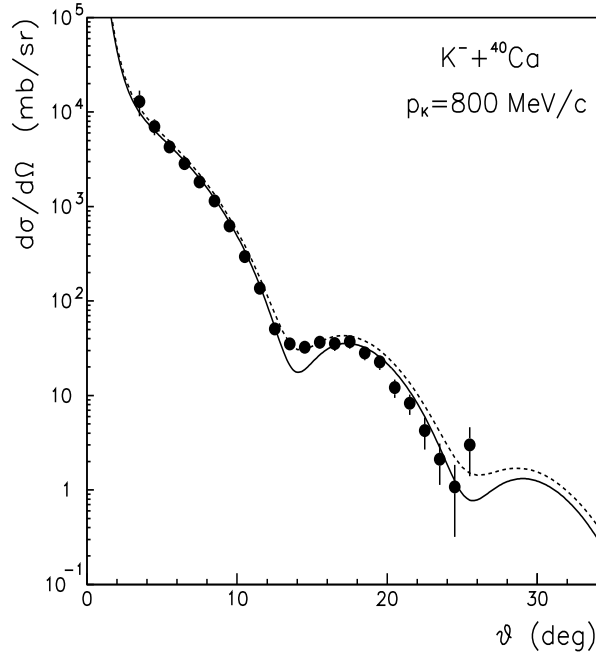


FIG. 2. The differential cross section for K^- elastic scattering from ^{40}Ca . The notations are the same as in Fig. 1.

Fig. 3 shows the K^-C elastic differential cross section calculated for ratios $\alpha=-0.1$ and $\alpha=-0.315$. The latter value for α was taken to be equal in magnitude to the parameter evaluated by the minimization procedure, but by substituting an opposite sign in order to demonstrate the sensitivity of the data to the sign of α .

TABLE I. The K^-N total cross section σ , ratio α of the real to imaginary part of the forward K^-N scattering amplitude and χ^2/N evaluated from the data on K^-A elastic scattering and that taken from the interaction in free space.

	evaluated from K^-A data [27]		taken from free K^-N interactions	
	^{12}C	^{40}Ca	^{12}C	^{40}Ca
α	0.315 ± 0.001	0.396 ± 0.003		0.608
σ	37.97 ± 0.01	38.3 ± 0.2		36.12

Now Fig. 3 illustrates that the absolute value of the ratio α might be reasonably fixed by the data. The calculations with $\alpha=-0.315$ provide a $\chi^2/N=2.3$, which is worse as compared to the value listed in Table I. Indeed, the data are sensitive to both sign and magnitude of the ratio α when taking into account the Coulomb scattering. This method has been used before for the evaluation of the real to imaginary ratio α in case of the antiproton-nucleon forward scattering amplitude in Refs. [26,29–32].

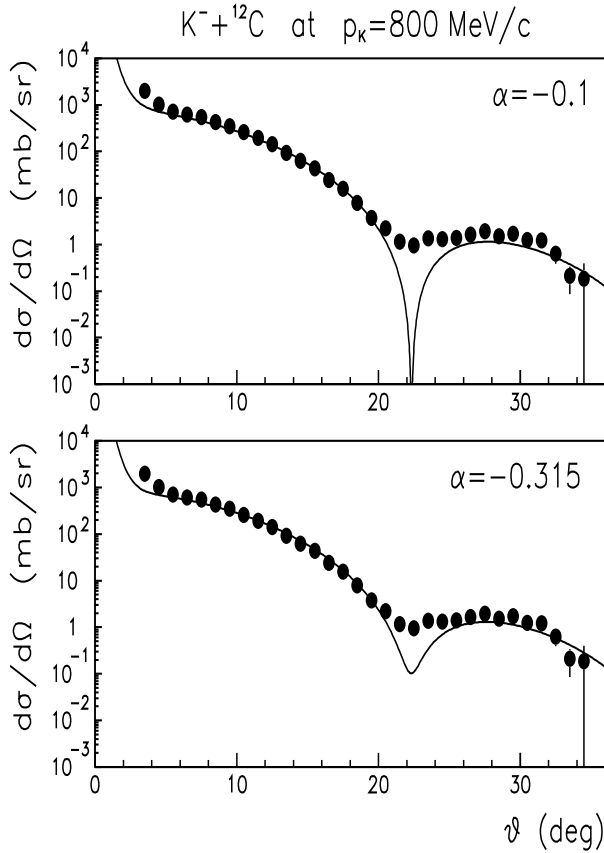


FIG. 3. The differential cross section for K^- elastic scattering from ^{12}C . The data are from Ref [27]. The lines show calculations with $\alpha=-0.1$ (upper part) and $\alpha=-0.315$ (lower part).

Since the inclusion of the Coulomb correction is important for the determination of the sign of α , we also have performed calculations taking into account only the nuclear phase shift. The results of this limit are shown in Fig. 4 for K^- scattering from ^{12}C and ^{40}Ca together with the data [27]. The parameters σ and α (extracted from the data) as well as the associated χ^2/N are also shown in Fig. 4. Note, that when neglecting the Coulomb correction the nuclear data become insensitive to the sign of α ; furthermore, for $\alpha=0$ the differential cross section in the diffractive minima will be zero.

From the analysis presented above it is clear, that without the Coulomb scattering it is not possible to reproduce

the data at low q . Although there are not much data available at small scattering angles, the Coulomb effect by obvious reason must be included in the data analysis. We also note that the calculations with the Coulomb effect yield the minimal χ^2/N .

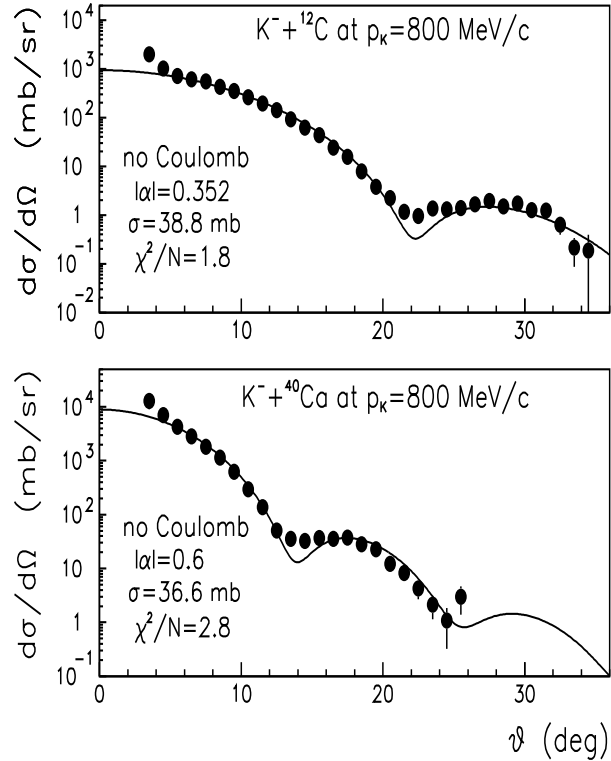


FIG. 4. The differential cross section for K^- elastic scattering from ^{12}C and ^{40}Ca . The data are from Ref [27]. The lines show calculations without the Coulomb correction. The parameters σ and α evaluated by Minuit [28] are shown in the figure together with the respective χ^2/N .

We conclude that the data [27] on elastic K^- -meson scattering from ^{12}C and ^{40}Ca nuclei are sufficiently sensitive to the evaluation of the in-medium total K^-N cross section σ and the ratio α of the real to imaginary part of the in-medium forward scattering amplitude $f(0)$. The resulting parameters are averaged over the proton and neutron numbers of the target. In the following these in-medium parameters will be compared to those extracted from the K^-N interaction in free space.

IV. WHAT DENSITIES CAN BE PROBED BY K^-A SCATTERING?

An important question in K^-A scattering is to what extent one can probe the nuclear interior. Obviously, for very peripheral scattering the values for σ and α should be sufficiently close to those values given by the K^-N

interaction in free space.

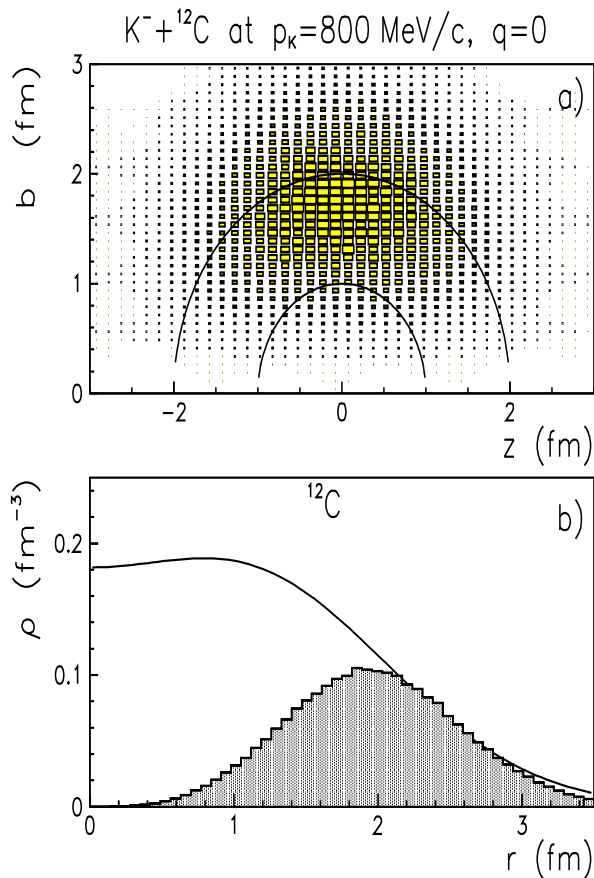


FIG. 5. a) The differential cross section for K^- elastic scattering from ^{12}C at an antikaon momentum $p_K=800$ MeV/c and $q=0$ as a function of the impact parameter b and coordinate z along the beam axis. The sizes of the granulated boxes are proportional to the cross section; the solid lines indicate radii of 1 and 2 fm. b) The solid line shows the density profile for ^{12}C while the histogram displays the scattering profile normalized to the density tail at large r .

Indeed, Eq. (1) indicates that elastic scattering is a peripheral process [33]. This is illustrated by Fig. 5a), where the differential cross section for K^- -meson scattering from ^{12}C at $\theta=0$ for an antikaon momentum of 800 MeV/c is shown as a function of the impact parameter b and the coordinate z along the beam axis (see Eq. (1)). The calculations show that the scattering is predominantly peripheral. To obtain the density probed by K^- scattering at this momentum we show (solid line in Fig. 5b)) the density profile for ^{12}C given by Eq. (10). The hatched histogram in Fig. 5b) indicates the K^-C scattering profile distribution, which was calculated by taking the K^-C elastic differential cross section at $p_K=800$ MeV/c and $q=0$ at given coordinates b and z and by integrating over the contour $r=\sqrt{b^2+z^2}$. The scattering profile is normalized to the tail of the density

function ρ .

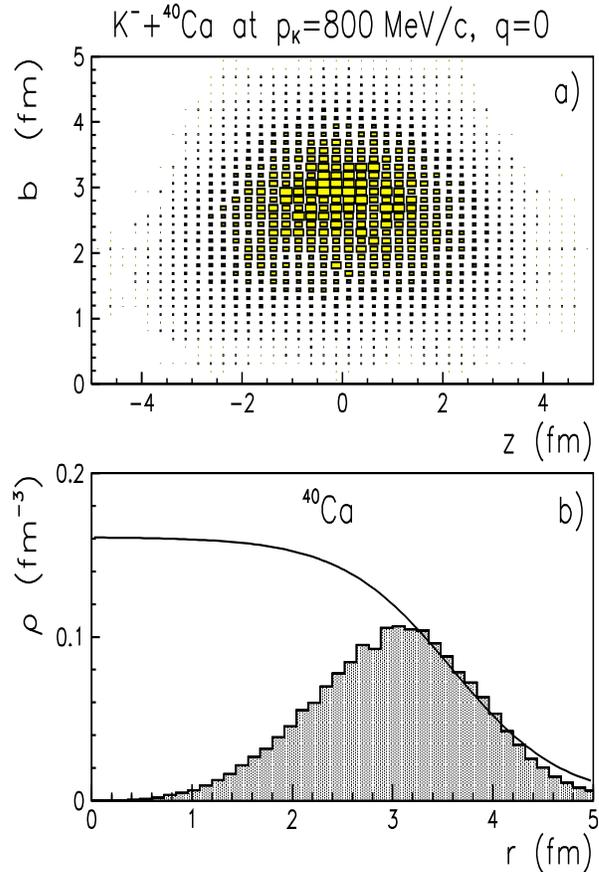


FIG. 6. Same as in Fig. 5 for K^- scattering from ^{40}Ca .

The maximal nuclear density that might be tested by K^- elastic scattering from ^{12}C is about $\simeq 0.1$ fm^{-3} , that should be compared to the saturation value $\rho_0=0.16$ fm^{-3} . The average densities probed by the K^- scattering are in the range of $\rho_0/3$. Similar conclusions also hold for the ^{40}Ca nucleus. This is demonstrated in Fig. 6 which shows the calculations of the reaction zone and the profile functions for K^- scattering from ^{40}Ca .

Now the in-medium modification of the total cross section σ and the ratio α of the real to imaginary part of the forward scattering amplitude and their difference from those values in free space might be discussed for the baryon densities probed in K^-A scattering.

V. THE K^-N FORWARD SCATTERING AMPLITUDE IN FREE SPACE

The forward K^- scattering amplitude on the proton and the neutron has been calculated in our previous study [18]. Here, we again evaluate the imaginary part of $f(0)$ from the available experimental data on the total cross section, while $\text{Re}f(0)$ is calculated by the dispersion

relations. The details of the calculations and references to related dispersion analyses are given in Ref. [18]. We directly continue with the status of the data and proper parameterizations.

Fig. 7 shows the experimental results [34] on the K^-p and K^-n total cross sections together with the parameterizations from Ref. [18]. Notice, that the data are well defined at $p_K=800$ MeV/c.

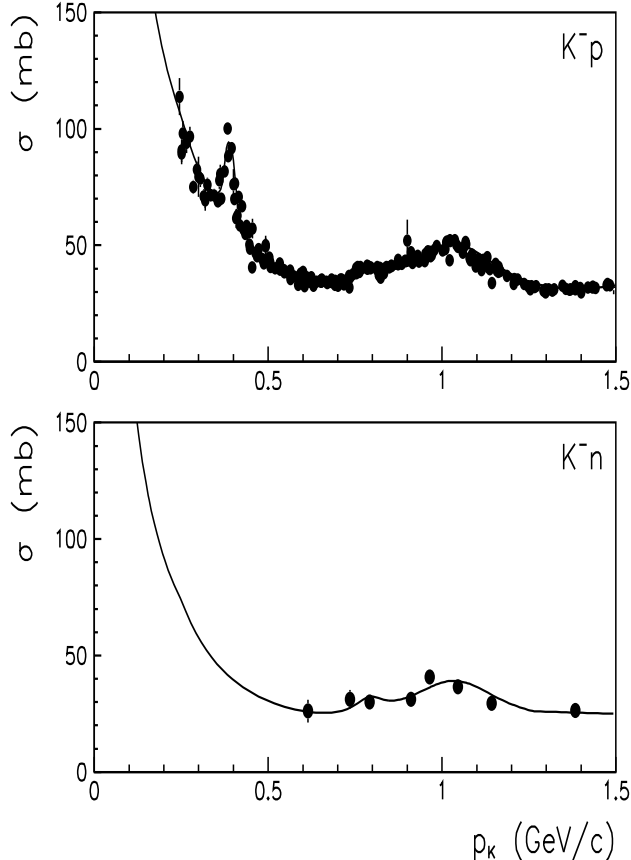


FIG. 7. The data on K^-p and K^-n total cross sections [34] together with the parameterizations from Ref. [18].

The resulting ratio $\alpha=Ref(0)/Imf(0)$ is shown in Fig. 8 as a function of the antikaon momentum for a proton and neutron target; the K^-p experimental results are taken from Refs. [35–37].

It is important to note, that the experimental result on the real part of the forward scattering amplitude is determined from

$$[Ref(0)]^2 = \left. \frac{d\sigma}{d\Omega} \right|_{q=0} - \left[\frac{k\sigma}{4\pi} \right]^2, \quad (13)$$

which does not provide the sign of α . However, the sign of $Ref(0)$ can be fixed by the combined data analysis with the K -matrix and the dispersion relations [38] by applying the crossing symmetry. We also note, that the

amount of experimental points shown in Fig. 8 for K^-p scattering is larger than that in the latest analysis by Martin [38].

The situation for the real part of the K^-n forward scattering amplitude is different. While $Re(f(0))$ can be reasonably determined from the low energy solution within the K -matrix analysis, there remains an uncertainty in the absolute normalization of the subtraction point. The latter one is fixed by the two experimental points [38] shown in the lower part of Fig. 8. However, the experimental results do not indicate the sign of $Ref(0)$.

Furthermore, there are no data available for the real part of the K^+n forward scattering amplitude. In principle, the ratio α for the K^-n scattering might stay positive and not change its sign around $p_K \simeq 1.2$ GeV. However, for these antikaon momenta the ratio α is small and close to zero. This important feature will be discussed later again.

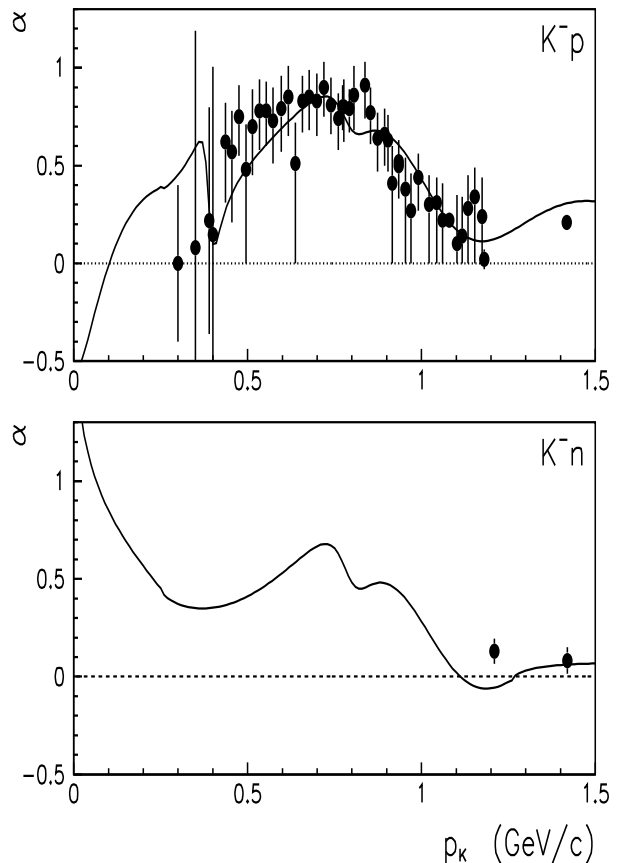


FIG. 8. The ratio α of the real to imaginary part for the K^-p and K^-n forward scattering amplitudes. The experimental results are taken from Refs. [35–38] while the solid lines show our calculations [18].

Keeping in mind the uncertainties in the determination of the ratio α for the K^-n interaction we now can perform a comparison with the data evaluated from the

VI. COMPARISON WITH THE DATA FROM K^- -A SCATTERING

Both, ^{12}C and ^{40}Ca , are isospin-symmetric nuclei and for a comparison with the values of σ and α in free space we average over the results from the previous section for proton and neutron targets. In principle, the cross section σ and the ratio α should be averaged over the Fermi distribution available at densities $\rho < 0.1 \text{ fm}^{-3}$, which is important for antikaon momenta where σ or α rapidly change with p_K . However, this is not the case for $p_K = 800 \text{ MeV}/c$.

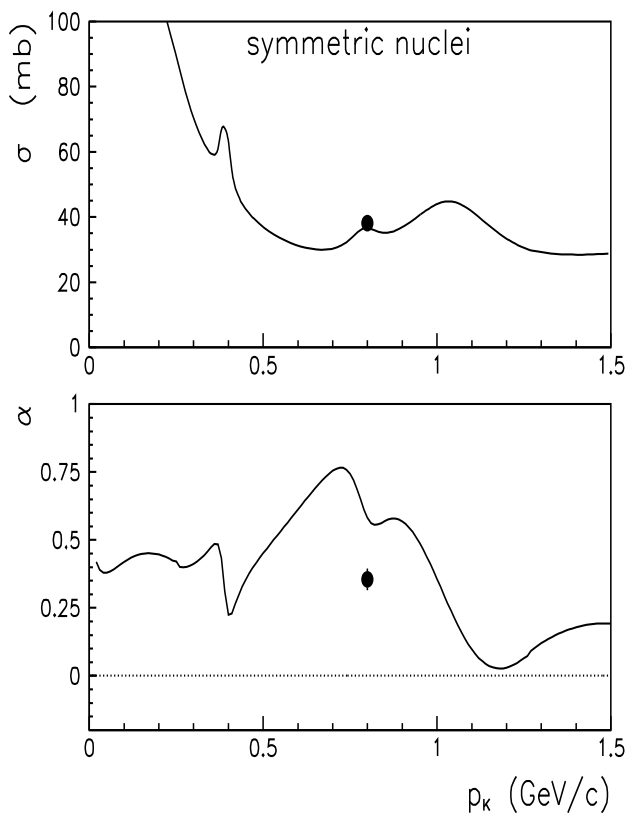


FIG. 9. The solid lines indicate the K^-N cross section σ and ratio α given in free space averaged over equal numbers of protons and neutrons. The solid circles show the results evaluated from the data on K^- elastic scattering from nuclei averaged over ^{12}C and ^{40}Ca .

The cross section σ and ratio α taken from the free K^-N interactions averaged over equal numbers of protons and neutrons are shown in Fig. 9 by the solid lines. The dots in Fig. 9 indicate the results evaluated from the data on K^- elastic scattering (see Table I) averaged over the ^{12}C and ^{40}Ca targets.

We find that the total cross section extracted from nu-

clear elastic scattering is practically equal to the value given in free space, while the ratio α differs by about a factor of $\simeq 1.5$. When discussing this difference one should keep in mind that the calculations actually do not reproduce the data exactly at the diffractive minima leaving room for an uncertainty in the ratio α , which is not well defined in free K^- -neutron interactions. The factor $\simeq 1.5$ might be attributed to the subtraction point providing a global shift of α (cf. Fig. 8). However, in this case the two experimental points [38] for the real part of the K^-n forward scattering amplitude cannot be reproduced. We thus reject this possibility.

Since the total K^-N cross section apparently is not modified in nuclear matter at densities $\rho < 0.1 \text{ fm}^{-3}$ and antikaon momenta of $800 \text{ MeV}/c$ relative to its value in free space, the drop in α should be attributed to a decrease of the real part of the forward K^-N scattering amplitude.

VII. THE K^- OPTICAL POTENTIAL

Adopting a spherically symmetric nuclear optical potential U_N the phase shift χ_N is given as [20]

$$\chi_N(b) = -\frac{m}{k} \int_{-\infty}^{\infty} U_N(b, z) dz. \quad (14)$$

Comparing to Eq. (2) this gives

$$U_N(r) = -\frac{2\pi f(0)}{m} \rho(r), \quad (15)$$

which can be rewritten in terms of σ and α as

$$U_N(r) = -k \sigma \frac{\alpha + i}{2m} \rho(r). \quad (16)$$

The Coulomb potential, furthermore, is given as [26]

$$U_C(r) = -4\pi Z e^2 \left[\frac{1}{r} \int_0^r \rho(x) x^2 dx + \int_r^{\infty} \rho(x) x dx \right], \quad (17)$$

where ρ is the density distribution.

Fig. 10 shows the resulting real and imaginary part of the nuclear potential and the Coulomb potential for K^- -meson scattering on ^{12}C and ^{40}Ca at an antikaon momentum of $800 \text{ MeV}/c$. The results for U_N are shown for σ and α as evaluated from the experimental data on the differential elastic cross section and given in Table I.

The Coulomb potential is very small, however, important for the description of the differential data on the K^- elastic scattering from nuclei. The imaginary part of the optical potential clearly dominates and is close to that expected from free-space calculations. The real part of the potential is attractive but smaller than expected from free-space calculations [18].

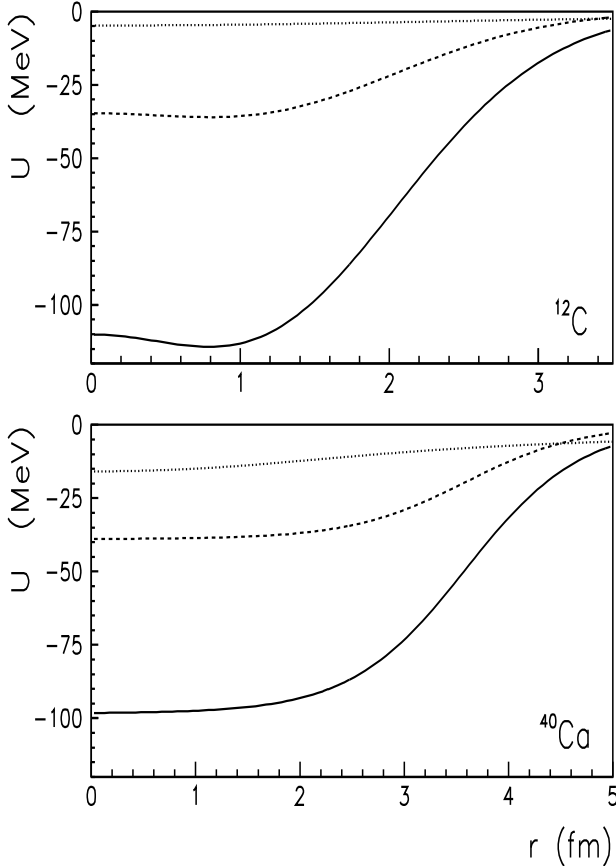


FIG. 10. The imaginary (solid) and real (dashed) nuclear potential and Coulomb potential (dotted line) for K^- scattering on ^{12}C and ^{40}Ca at an antikaon momentum of 800 MeV/c.

VIII. FURTHER PERSPECTIVES

In this Section we outline further perspectives of experiments on differential data for K^- elastic scattering from nuclei. There are two regions of antikaon momenta that are crucial for the understanding of the K^- properties in nuclear matter and which can be studied by K^- -meson elastic scatterings from nuclei at densities $\rho < 0.1 \text{ fm}^{-3}$. Let us discuss both of them by starting with the high energy region.

A. Antikaon momenta around 1.2 GeV/c

As shown in Fig. 8 the ratio α of the real to imaginary part of the forward scattering amplitude in free K^- -neutron interactions is close to zero for antikaon momenta of $\simeq 1.2 \text{ GeV}/c$. After averaging of α over the number of protons and neutrons in the target the average $\alpha \approx 0$ remains. The result for symmetric nuclei is shown in Fig. 9.

We recall that neglecting Coulomb scattering the calculations with $\alpha=0$ yield a differential elastic cross section which is exactly equal to zero at the diffractive minima. Taking into account the interference between the nuclear and Coulomb phase shifts the α -dependence of the cross section in the vicinity of the diffractive minima becomes more complicated [26], but can be predicted using σ and α given in free space.

Fig. 11 shows the differential elastic cross section for K^- -meson scattering from ^{12}C at $p_K=1.2 \text{ GeV}/c$ calculated with $\sigma=33.8 \text{ mb}$ and $\alpha=0.02$, which corresponds to K^-N interactions in free space averaged over the number of protons and neutrons.

The calculations indicate a deep diffractive minimum due to the small value of the ratio α . We do expect that the measurements should allow to extract the actual value of α and its sign. This is important for the in-medium modification of the real part of the forward scattering amplitude $f(0)$ as well as for a possible change of sign of $\text{Re}f(0)$ around $p_K \simeq 1.2 \text{ GeV}$ for the K^-n interaction.

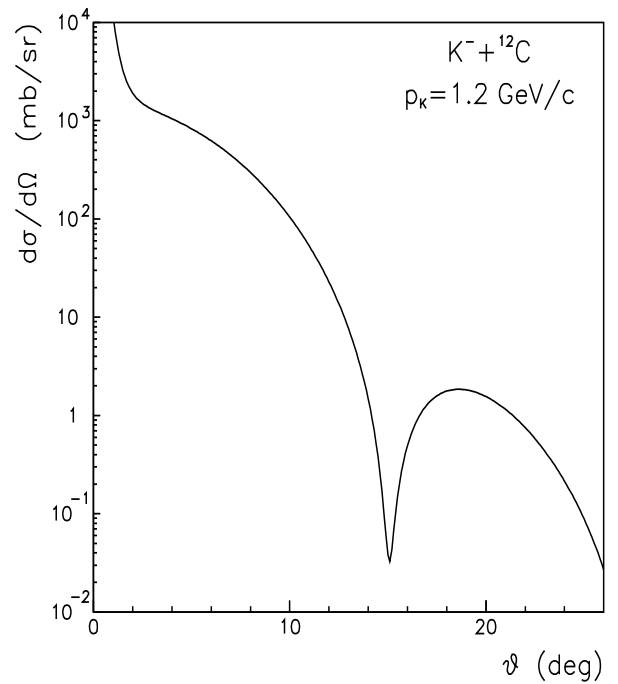


FIG. 11. The predicted differential cross section for K^- elastic scattering from ^{12}C at an antikaon momentum of 1.2 GeV/c.

A more sophisticated analysis can be done by scanning the antikaon momentum from 0.7 GeV/c to 1.4 GeV/c and a determination of the differential cross section at the first diffractive minimum, i.e. at its minimal point within the experimental resolution. As shown for the case of symmetric nuclear matter in Fig. 9 the cross section σ does not vary very much for antikaon momenta in this range while the ratio α strongly depends on p_K .

Fig. 12 shows the differential cross section at the first diffractive minimum for K^- elastic scattering from ^{12}C in the antikaon momentum range $0.7 \leq p_K \leq 1.4$ GeV. The solid line indicates the calculations performed with σ and α taken from the free space K^-N scatterings. The calculations are averaged at the diffractive minimum over the scattering angles with $\Delta\theta = \pm 0.05$ degrees. The full dot in Fig. 12 shows the experimental result from Ref. [27] while the result evaluated by the χ^2 minimization is shown in terms of the full square at 0.8 GeV/c. Since the predicted differential cross section at the diffractive minimum substantially depends on the antikaon momentum (by two orders of magnitude) we expect that the measurements should indicate a strong variation of $d\sigma/d\Omega$ even within the systematical uncertainties.

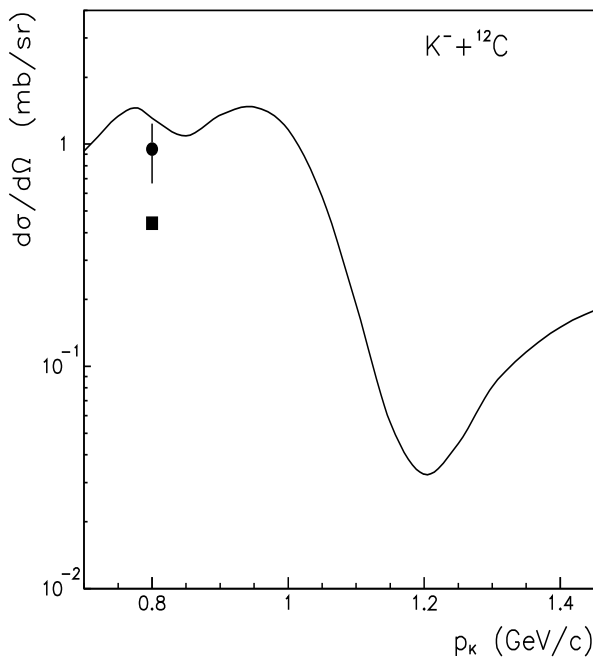


FIG. 12. The solid line shows the predicted differential cross section at the first diffractive minimum for K^- elastic scattering from ^{12}C as a function of the antikaon momentum. The calculations are performed with σ and α given in free space. The circle shows the experimental result from Ref. [27] while the full square shows the result from our fitting procedure at 0.8 GeV/c.

B. Antikaon momenta below 400 MeV/c

Fig. 8 indicates that in free space the real part of the forward scattering amplitude close to zero antikaon momenta is negative for K^-p and positive for K^-n interactions. By taking the free space values the real part of the optical potential for isospin symmetric nuclei amounts to $\simeq -18$ MeV at $p_K=0$. Thus the real part of U_N is attractive, but small, which contradicts the experimental

data on kaonic atoms where a depth of the K^- potential at ρ_0 of -180 MeV [6,7] has been extracted. This discrepancy was resolved in the literature by considering the in-medium modification [39–42] of the $\Lambda(1405)$ resonance which couples to the K^-p channel and yields a negative $f(0)$ in free space at low antikaon momenta. The dominant effect, which modifies the $\Lambda(1405)$ dynamics in nuclear matter, stems from the Pauli blocking of the intermediate nucleon states which causes a dissolution of this resonance [43,44] and an in-medium modification of the K^-p forward scattering amplitude. For the most recent review of the problem as well as the current status on the analysis of kaonic atoms the reader is referred to Ref. [45].

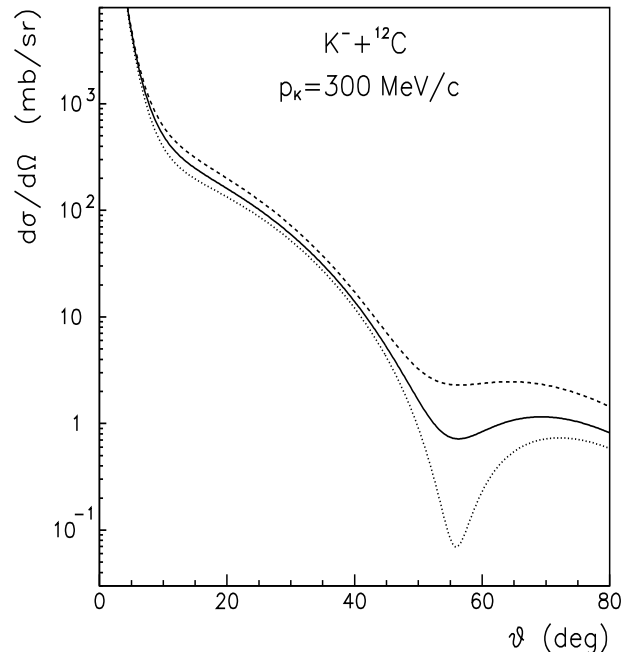


FIG. 13. The differential cross section for K^-C elastic scattering at $p_K=300$ MeV/c. The solid line shows the calculation with σ and α taken from free space, the dotted line shows the result for $\alpha=0$, respectively. The dashed line represents a calculation where the contribution from the $\Lambda(1405)$ resonance to the total real part of $f(0)$ is discarded.

The contribution from the $\Lambda(1405)$ resonance to the total real part of the K^-p forward scattering amplitude is sizeable up to antikaon momenta of $\simeq 400$ MeV/c [18]. Thus the in-medium modification of $f(0)$ might also be studied by K^- elastic scattering from nuclei at low antikaon momenta $p_K < 400$ MeV/c. However, the crucial question here is the validity of the Glauber theory at low energies. The limits of its applicability as well as the analysis of data on low energy antiproton elastic and inelastic scatterings from nuclei are given in Ref. [26]. It follows that Glauber theory at low energies may serve only as a leading consideration.

Fig. 13 shows the differential cross section for K^- elastic scattering from ^{12}C at an antikaon momentum of 300 MeV/c. The solid line indicates a calculation with cross section σ and ratio α taken from the free space K^-N interactions while the dotted line shows the result obtained with the same σ but for $\alpha=0$.

The dashed line in Fig. 13 shows the calculation with the modified real part of the forward K^-p scattering amplitude by discarding the contribution from the $\Lambda(1405)$ resonance to $\text{Re}f(0)$. In the latter case we obtain $\alpha=0.82$ after averaging over protons and neutrons.

Fig. 13 indicates that the difference between the calculations with different ratios α is sizeable. Although our predictions at $p_K=300$ MeV/c may serve only as a leading extrapolation, we expect that the effect of the in-medium modification of the forward scattering amplitude can actually be measured by elastic K^-A scattering.

IX. CONCLUSIONS

In this work we have considered the possibility to extract the antikaon potential from differential data on elastic K^-A scattering within the Glauber theory and analyzed the experimental results [27] for K^- elastic scattering from ^{12}C and ^{40}Ca at an antikaon momentum of 800 MeV/c. We have found that the total K^-N cross section extracted from the data is close to the value given in free space K^-p and K^-n interactions when averaged over the number of protons and neutrons in the target. On the other hand, the ratio α of the real to imaginary part of the forward scattering amplitude $f(0)$ - as evaluated from the data - differs from the ratio α in free space. Since the imaginary part of $f(0)$ seems not to be modified this difference indicates an in-medium modification of the real part of $f(0)$. However, the confidence level of this result (within the χ^2 method) is below 10% which leaves it as an indication and does not allow for a final conclusion. The parameters evaluated from K^- scattering from ^{12}C and ^{40}Ca have been used for a reconstruction of the antikaon potential at $p_K=800$ MeV/c, which is found to be attractive in line with the analysis from Kiselev [46] at 1.2 GeV/c.

We have investigated the target nuclear densities that can be tested by K^-A elastic scattering and found them to range from 0 to $\rho=0.1$ fm $^{-3}$. To extrapolate the depth of the K^- potential at $\rho\simeq 0.17$ fm $^{-3}$ we have used nuclear density profiles with parameters evaluated from electron-nucleus scattering.

Furthermore, we collect the information on the real part of the antikaon potential from all available sources for different antikaon momenta and show the results in Fig. 14 extrapolated to normal nuclear density $\rho=0.17$ fm $^{-3}$. The potential $\text{Re}U_N=180\pm 20$ MeV at $p_K=0$ stems from the data on kaonic atoms [6,7,45] with the most recent analysis performed in Ref. [45]. The analysis of the experimental results [8–12] on K^- -

meson production from heavy-ion collisions is taken from Refs. [13–17] and indicates $\text{Re}U_N=-80\div 120$ MeV at antikaon momenta $300\leq p_K\leq 600$ MeV/c. Fig. 14 also shows the potential evaluated in this work from the data on K^-C and K^-Ca elastic scattering; the indicated error-bar is due to a standard deviation corresponding to a 5% confidence level. Moreover, the solid line in Fig. 14 shows our result from Ref. [18] calculated by discarding the contribution from $\Lambda(1405)$ and $\Sigma(1385)$ resonances at nuclear matter density. Note that the experimental results as well as the calculations indicate an attractive K^- potential up to antikaon momenta of $\simeq 1.3$ GeV/c.

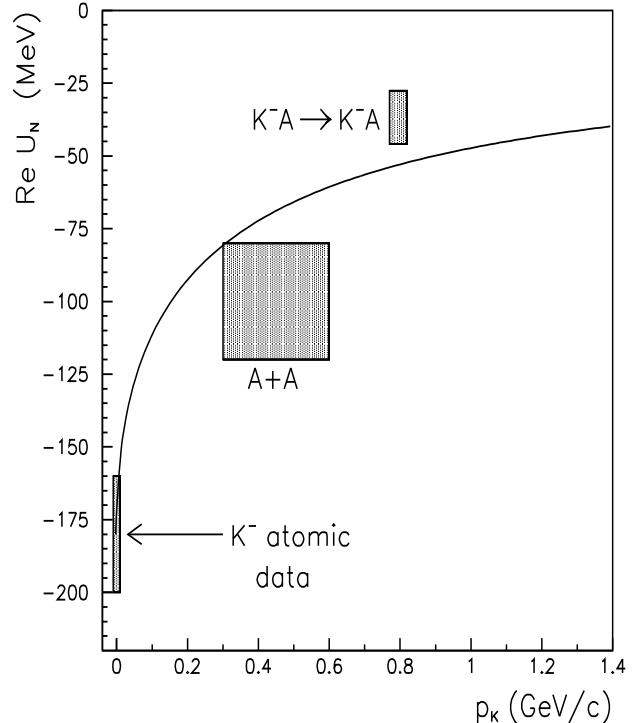


FIG. 14. The real part of the optical antikaon potential at baryon density $\rho=0.17$ fm $^{-3}$ as a function of the K^- -meson momentum. The potential $\text{Re}U_N$ from the K^- atomic data is taken from the recent analysis of Ref. [45]. The potential denoted by $A+A$ has been extracted from K^- data on heavy-ion collisions [8–12] and is taken from Refs. [13–17]. The potential evaluated from $K^-A\rightarrow K^-A$ elastic scattering at 0.8 GeV/c is the result of the present study. The solid line shows our calculation from Ref. [18].

We, furthermore, have discussed future perspectives in K^-A elastic scatterings and the investigation of the antikaon potential or modification of the scattering amplitude $f(0)$. It is pointed out that K^-A elastic scattering at low antikaon momenta may provide an additional (obvious) way to reconstruct the antikaon potential as an alternative to heavy-ion and proton-nucleus [18,47–51] studies. Furthermore, measurements of the elastic K^- scattering from nuclei at $p_K\simeq 1.2$ GeV/c provide an effective tool to investigate, if the real part of the K^-n for-

ward scattering amplitude changes its sign around this momentum, and to learn more about the interaction between the antikaon and neutron.

-
- [1] D.B. Kaplan and A.E. Nelson, Phys. Lett. B **175**, 57 (1986)
- [2] G.E. Brown and M. Rho, Phys. Rev. Lett. **66**, 2720 (1991).
- [3] G.E. Brown, Phys. Blätter **53**, 671 (1997).
- [4] V. Thorsson, M. Prakash and J.M. Lattimer, Nucl. Phys. A **572**, 693 (1994); A **574**, 851 (1994).
- [5] J. Schaffner, A. Gal, I.N. Mishustin, H. Stöcker and W. Greiner, Phys. Lett., B **334**, 268 (1994).
- [6] E. Friedman, A. Gal and G. Batty, Phys. Lett. B **308**, 6 (1993).
- [7] E. Friedman, A. Gal and G. Batty, Nucl. Phys. A **579**, 518 (1994).
- [8] A. Schröter et al., Z. Phys. A **350**, 101 (1994).
- [9] P. Senger et al., Acta Phys. Pol. B **27**, 2993 (1996).
- [10] R. Barth et al., Phys. Rev. Lett. **78**, 4007 (1997).
- [11] F. Laue et al., Phys. Rev. Lett. **82**, 1640 (1999).
- [12] P. Senger and H. Strobele, J. Phys. G **25**, R59 (1999).
- [13] G.Q. Li, C. M. Ko and X.S. Fang, Phys. Lett. B **329**, 149 (1994).
- [14] W. Cassing et al., Nucl. Phys. A **614**, 415 (1997).
- [15] G.Q. Li, C.H. Lee and G.E. Brown, Nucl. Phys. A **625**, 372 (1997).
- [16] E. L. Bratkovskaya, W. Cassing and U. Mosel, Nucl. Phys. A **622**, 593 (1997); Phys. Lett. B **424**, 224 (1998).
- [17] W. Cassing and E. L. Bratkovskaya, Phys. Rep. **308**, 65 (1999).
- [18] A. Sibirtsev and W. Cassing, Nucl. Phys. A **641**, 476 (1998).
- [19] A. Sibirtsev and W. Cassing, nucl-th/9909024.
- [20] R.J. Glauber, *Lectures in Theoretical Physics*, Interscience Publishers, New York (1959) p.315.
- [21] R.G. Newton, *Scattering Theory of Waves and Particles*, Springer-Verlag, Berlin (1982) p.605.
- [22] W. Czyz, L. Lesniak and H. Woleck, Nucl. Phys. B **19**, 125 (1970).
- [23] R.J. Glauber and G. Matthiae, Nucl. Phys. B **21**, 125 (1970).
- [24] I. Ahmad, Nucl. Phys. A **247**, 418 (1975).
- [25] G.D. Alkhasov, S.L. Belostotsky and A.A. Vorobyov, Phys. Rept. C **42**, 89 (1978).
- [26] O.D. Dalkarov and V.A. Karmanov, Nucl. Phys. A **445**, 579 (1985).
- [27] D. Marlow et al., Phys. Rev C **25**, 2619 (1982).
- [28] F. James and M. Roos, Comp. Phys. Commun. **10**, 343 (1975).
- [29] O.D. Dalkarov and V.A. Karmanov, Phys. Lett. B **147**, 1 (1984).
- [30] M. Cresti, L. Peruzzo and G. Sartori, Phys. Lett. B **132**, 209 (1983).
- [31] R. Clapisch, Nucl. Phys. A **434**, 222 (1985)
- [32] H. Iwasaki et al., Phys. Lett. B **103**, 247 (1981).
- [33] L.A. Kondratyuk and Yu. Simonov, JETP Let. **17**, 435 (1973).
- [34] Particle Data Group, Eur. Phys. J. C **3**, 1 (1998).
- [35] B. Conforto et al., Nucl. Phys. B **8**, 263 (1968).
- [36] R. Armenteros et al., Nucl. Phys. B **21**, 13 (1970).
- [37] O.V. Dumbrajs, T.Yu. Dumbrajs and N.M. Queen, Fortschr. Phys. **19**, 491 (1971).
- [38] A.D. Martin, Nucl. Phys. B **179**, 33 (1981).
- [39] V. Koch, Phys. Lett. B **337**, 7 (1994).
- [40] T. Waas, M. Rho and W. Weise, Nucl. Phys. A **617**, 449 (1997).
- [41] A. Ohnishi, Y. Nara and W. Koch, Phys. Rev. C **56**, 2767 (1997).
- [42] M. Lutz, Phys. Lett. B **426**, 12 (1998).
- [43] G.E. Brown and M. Rho, Nucl. Phys. A **596**, 503 (1996).
- [44] T. Waas, W. Weise, Nucl. Phys. A **625**, 287 (1997).
- [45] E. Friedman, A. Gal, J. Mareš and A. Cieplý, nucl-th/9804072.
- [46] Yu. T. Kiselev et al., J. Phys. G **25**, 381 (1999).
- [47] T. Kirchner et al., COSY Proposal 21;
- [48] K. Sistemich et al., Strangeness in nuclei, Krakow (1992) p.359.
- [49] O.W.B. Schult et al., Nucl. Phys. A **583**, 629c (1995).
- [50] A. Sibirtsev, H. Müller and C. Schneidereit, Z. Phys. A **351**, 333 (1995).
- [51] M. Büscher et al., Acta Phys. Pol. **27**, 3087 (1996).